

EXPERIMENTAL AND ANALYTICAL EVALUATION OF THE MODAL PARAMETERS CHANGES OF A LARGE TELESCOPIC STRUCTURE

R.L. Boroschek¹ and F.J. Hernández²

¹ Associate Professor, Dept. of Structural Engineering, University of Chile, Santiago, Chile.

² Engineering Student, Dept. of Structural Engineering, University of Chile, Santiago, Chile.

Email: rborosch@ing.uchile.cl, fraherna@ing.uchile.cl

ABSTRACT :

Experimental and analytical estimation of changing modals parameters of a 132 meters long telescopic 3D frame ship loading structure is presented. The structure consist of an external 110 meters length 3D steel truss than can move in the horizontal plane and an internal 3D trust that works as extending arm. The amount of arm extension changes continuously according to ship position and loading conditions. Due to the redistribution of mass and rigidity, the modal parameters of the structure changes continuously. To capture the space - frequency characteristic time - frequency system identification techniques were evaluated and presented in this paper: Short Time Frequency Spectrum, the Hilbert-Huang Transform (HHT) and the Wigner-Ville Distribution (WVD). Also an analytical model is used to describe the dynamic behavior of the structure to evaluate the identification methods.

KEYWORDS: Time-Frequency Analysis, Wigner-Ville Distribution, Spectrogram, Hilbert-Huang Transform, System Identification.

1. INTRODUCTION

In this article a dry material ship loader vibration data is presented. Loading material is carried by conveyor belts and later dumped, using a specialized discharge system, Figure 1(a). The ship loader structure consist of an external 110 meters length 3D steel truss than can move in the horizontal plane and an internal 3D trust that works as an extending arm. The total combined length of the structure after full extension of the telescopic arm is approximately 132 meters. The structure can rotate approximately 60 degrees in the horizontal plane. To stabilize the structure a large concrete weight is located at the ground side. Basic geometry of the structure is shown in Figure 1(a). The typical sections used are wide flange, which have been reinforced in some parts with additional channel elements. The total weigh of the empty structure is approximately 5500 kN.

Due to dock characteristics the telescopic arm position changes continuously, according to ship position and loading condition. The radial and tangential position of the loading end is change by an operator located on the free end of the telescopic arm, just above the ship loading area.

The telescopic arm is supported on the main structure by mean of 8 wheels, with bottom and top rails attach to outer structure. Top and bottom railing are separated by a distance slightly greater than the wheel diameter. This generates a single contact surface per wheel axis, top or bottom, depending on the telescopic arm position and loading characteristics. This gap an others structural conditions allow the telescopic arm to vibrate with relative large amplitudes when the loading discharge rate and structural modes are close enough to resonance.

2. VIBRATION TESTING

Vibration testing of the structure had to be done with a maximum of 12 hours time and during loading of a single

material type. Due to operation conditions and safety of the personnel only seven sensors were allowed to be placed on top of the structure, Figure 1(b).

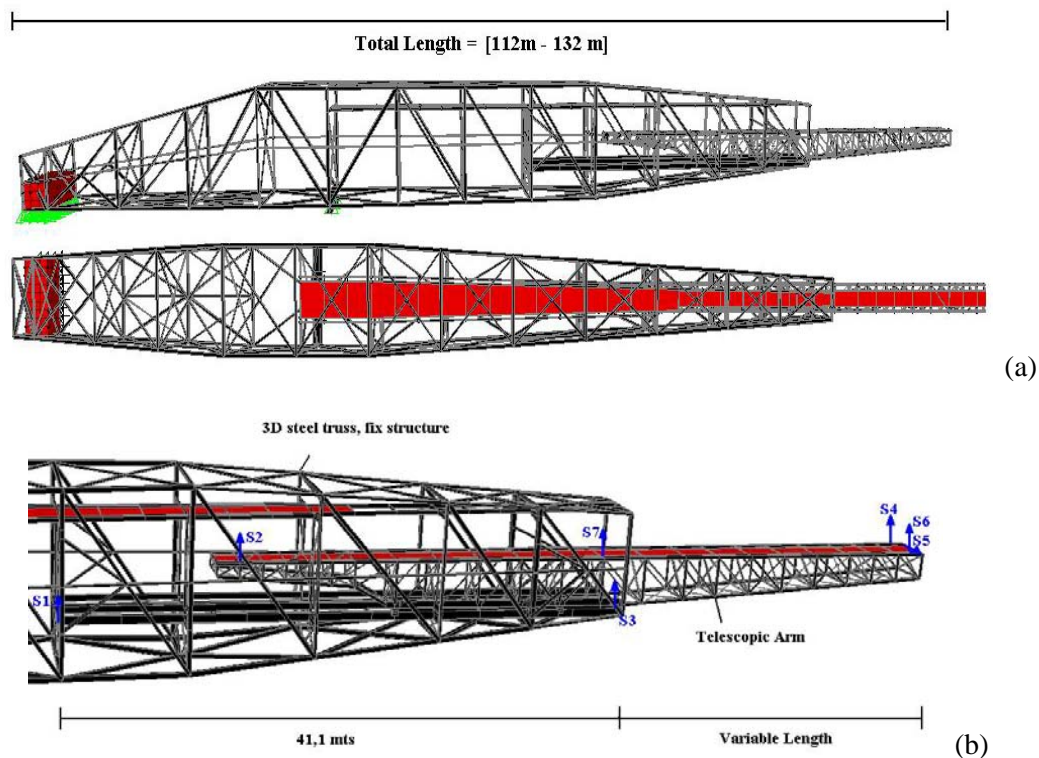


Figure 1: (a) 3-D Structure, (b) Sensor Location.

Ambient vibration and impact tests were performed at five different telescopic arm extensions, Table 1. For this test the structure was extended, enough time was left to reduce transient response and latter ambient recording was performed. Additionally impact tests were generated on the structure by jumping close to each sensor location. To compare the static with dynamic changes of the modal parameters, forward and backward motion of the telescopic arm was monitored. Finally vibration data for different loading rates of dry material was measured. Loading rate monitored varied from 6000 to 10000 kN/hour in steps of 1000 kN/hour. In addition to vibration measurement, vibration perception was indicated by the operator located at the control cabin.

3. ANALYSIS OF LINEAL STRUCTURE FOR DIFFERENT ARM POSITION.

Several ambient vibration records were obtained for different telescopic arm positions. Results are presented in more detail in Boroschek and Hernandez (2007).

Ambient vibrations were monitored at different telescopic arm extensions, 4.6, 9.6, 13.6, 18.5 and 22.4 meters. For each position, vibrations were recorded after the transient signal due to the extension of the arm had substantially decayed. Power Spectral Density (PSD) for different positions is presented for a vertical sensor located next to the control cabin, (end arm) for two principal modes, Figure 2 and Figure 3. The PSD in these figures has been normalized. The predominant frequencies determined from the different positions and loading conditions are shown in Table 1. Frequency variations during different loading rates are close to 8%, for loading rates of 0 to 10000 kN/hour.

Several important features can be observed from figures and table:

1. The predominant frequency of the transverse motion varies from 0.64 to 0.71 Hz.
2. The predominant frequency of the vertical motion of the complete structure varies from 0.85 to 0.94 Hz. The motion associated with this frequency, also has contribution in the horizontal plane, although they

are smaller than in the vertical direction.

- The second predominant vertical motion is mainly govern by the vibration of the telescopic arm (1.5 Hz).

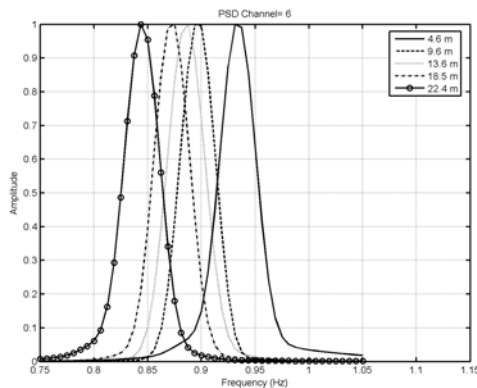


Figure 2: Power Spectral Density Frequency Variation as a Function of Position. Lower Frequency. Sensor 6.

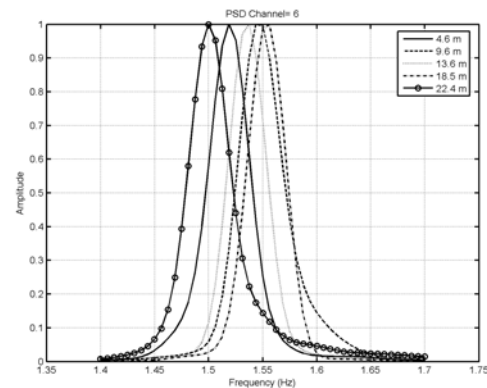


Figure 3: Power Spectral Density Frequency Variation as a Function of Position. Higher Frequency. Sensor 6.

- An important characteristic of the motion is that when the arm is extending, the main predominant vertical frequency diminishes, as seen in Figure 2. The larger the extension the larger the reduction in predominant frequency. (0,93 to 0,84 Hz).
- On the contrary the second predominant vertical vibration that is dominated mainly by the telescopic arm does not have a proportional change with arm extension, Figure 3. For example for 4.6 meter predominant frequency is close to 1.52 Hz, for 18.5 meters predominant frequency is 1.55 Hz and for 22.4 m frequency is 1.50 Hz. These are not large variations for resonance study purposes, but large enough to be detected with this rather crude method. The reason for this non proportionality is because the telescopic arm is supported on wheels that move on rails that are supported every 6,9 or 9,1 meters by the vertical elements of the non telescopic framing structure. When the wheels are close to a vertical element then the rigidity of the railing systems increases, modifying the predominant frequency. In case that the telescopic arm was supported on an infinite rigid railing system, then its predominant frequency will not change. The importance of main external structure on this predominant vertical frequency is rather small, except for the local stiffness of its connecting elements.

4. CONTINUOUS MONITORING OF PREDOMINANT FREQUENCY VARIATIONS

An interesting aspect of this study is the possibility of continually monitor the predominant frequency variations of the system. There are several methods to estimate the frequency variation as a function of time. The simplest one is the Short Time Fourier Transform (Cohen, 1995) and its squared value the spectrogram. This procedure plots a short time window Fourier Transform of the data in a sequential form, generating an estimate of amplitude, frequency and time. Figure 4 presents a vibration record and its spectrogram, obtained when the telescopic arm was extended from 4.6 to 22.4 meters, in 40 seconds. The two predominant vertical frequencies are clearly observed. Figure 5 presents a spectrogram of a band filter signal around the lower vertical predominant frequency (LF). A solid black line has been drawn following the maximum values. A clear frequency variation is observed from seconds 25 to 60 in the record. This value agrees with which was observed from the fix position measurement of the telescopic arm, Figure 6 presents the frequency band corresponding to the second vertical predominant motion (HF). In this case as observed previously, a clear tendency is not present, nevertheless variation are rather small. When the telescopic arm is contracted an inverse trend is observed.

Table 1: Predominant Frequency

Extension 4.6 m		
Direction	Frequency [Hz]	Frequency Analytic Model Unloaded Structure [Hz]
Horizontal	0.667	0.78
Vertical	[0.933 - 0.938]	0.91
Vertical	[1.537 - 1.545]	1.62
Horizontal	[1.985 - 1.990]	1.63
Extension 9.6 m		
Direction	Frequency [Hz]	Frequency Analytic Model Unloaded Structure [Hz]
Horizontal	[0.661 - 0.644]	0.74
Vertical	[0.896 - 0.897]	0.87
Vertical	[1.546 - 1.549]	1.57
Horizontal	[2.023 - 2.027]	1.59
Extension 13.6 m		
Direction	Frequency [Hz]	Frequency Analytic Model Unloaded Structure [Hz]
Horizontal	[0.705 - 0.712]	0.73
Vertical	[0.866 - 0.887]	0.85
Vertical	1.535	1.60
Horizontal	[2.102 - 2.107]	1.64
Extension 18.5 m		
Direction	Frequency [Hz]	Frequency Analytic Model Unloaded Structure [Hz]
Horizontal	[0.680 - 0.686]	0.69
Vertical	[0.871 - 0.873]	0.83
Vertical	[1.554 - 1.556]	1.61
Horizontal	2.149	1.59
Extension 22.4 m		
Direction	Frequency [Hz]	Frequency Analytic Model Unloaded Structure [Hz]
Horizontal	[0.643 - 0.652]	0.67
Vertical	[0.845 - 0.899]	0.80
Vertical	1.502	1.55
Horizontal	[2.108 - 2.110]	1.58

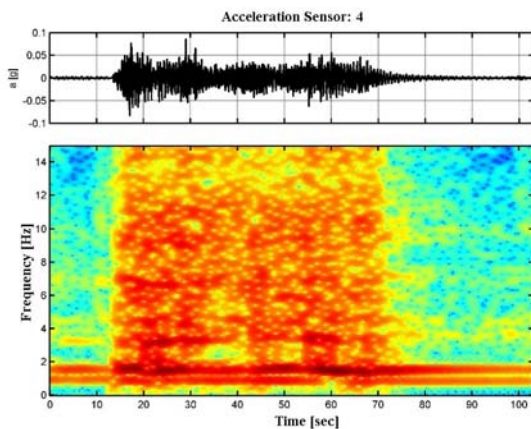


Figure 4: Spectrogram Vertical Acceleration, Sensor 4. Telescopic Arm Extension.

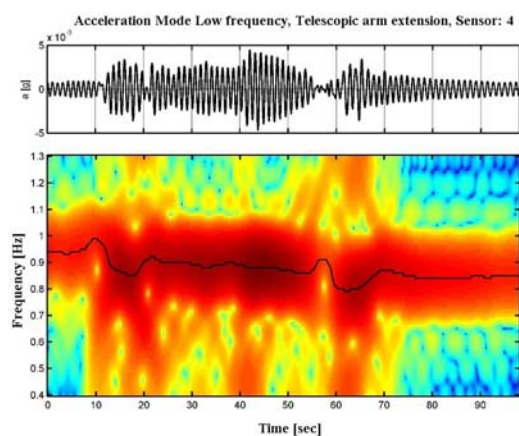


Figure 5: Spectrogram Vertical Acceleration, Sensor 4. Telescopic Arm Extension. LF.

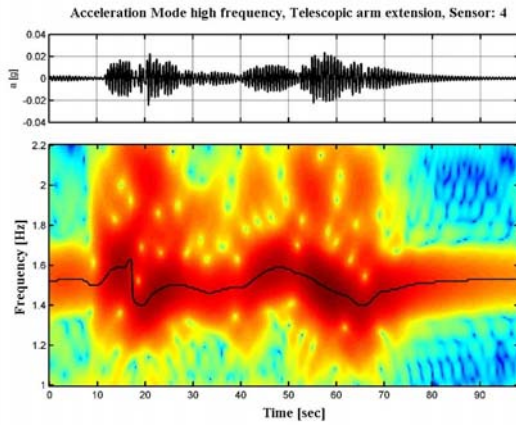


Figure 6: Spectrogram of Vertical Acceleration of Sensor 4. Telescopic Arm Extension. HF.

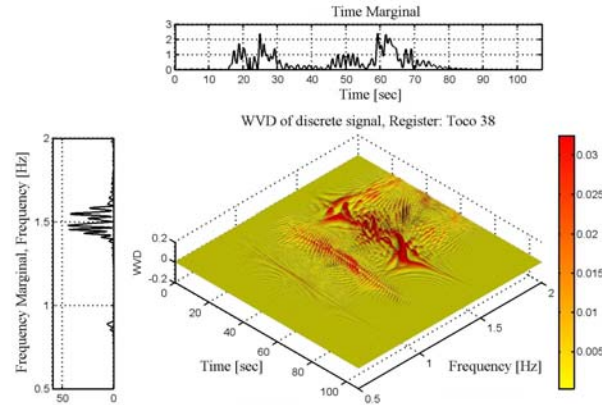


Figure 7: Wigner-Ville Distribution of Vertical Acceleration of Sensor 4.

The Wigner-Ville distribution of a signal ($x(t)$) is defined by (Ville, 1948, Cohen, 1995):

$$WV(t, w) = \frac{1}{2\pi} \int_{-\infty}^{\infty} x^* \left(t - \frac{1}{2} \tau \right) x \left(t + \frac{1}{2} \tau \right) e^{-j\tau w} d\tau \quad (4.1)$$

The Wigner-Ville distribution of acceleration record shown in Figure 4 can be seen in Figure 7. The signal on the 0.8 - 0.95 frequency band is present with relative low amplitude. The second predominant vertical frequency, close to 1.5 Hz is clearly visible and defined. The frequency around 1.2 Hz is product of interference of the two signals. If the original acceleration record is low pass filtered, so that only the first predominant frequency is present and the maximum value of frequency for each time step is selected, a good estimate of the instantaneous frequency of the signal is found, Figure 10. There are several procedures to reduce the interference signal; nevertheless in some cases they reduce the location of the frequency change so they are not considered in this article.

The Hilbert-Huang Transform (HHT) (Huang et al. 1998) is a relative new technique. The HHT has two main steps; I) Empirical Mode Decomposition (EMD), and II) Hilbert Spectral Analysis. In the EMD process, the analyzed signals are adaptively decomposed into a finite number of Intrinsic Mode Functions (IMFs). An IMF is described as a function satisfying the following conditions: a) the number of peaks and the number of zero-crossing must either equal or differ at most by one; and b) at any point, the mean value of envelope defined by local maxima and the envelope defined by local minima is zero. An IMF defined as above is a nearly a monocomponent signal and should admits “well-behaved” Hilbert Transform. In order to obtain the frequency variation in the record, we used the analytical signal of each IMF. The analytical signal ($z(t)$) of a signal ($s(t)$) is defined as:

$$z(t) = 2 \cdot \frac{1}{\sqrt{2 \cdot \pi}} \cdot \int_0^{\infty} S(\omega) \cdot e^{j \cdot \omega \cdot t} \partial \omega = s(t) + j \cdot \underbrace{\frac{1}{\pi} \cdot \int_{-\infty}^{\infty} \frac{s(t')}{t - t'} \partial t'}_{H[s(t)], \text{ Hilbert Transform}} = a(t) \cdot e^{j \cdot \theta(t)} \quad (4.2)$$

$$\text{where } a(t) = \sqrt{s(t)^2 + (H[s(t)])^2}, \quad \theta(t) = \arctan \left(\frac{H[s(t)]}{s(t)} \right), \quad \omega(t) = \frac{\partial \theta(t)}{\partial t} \quad (4.3)$$

Where $a(t)$ and $\theta(t)$ is defined as the instantaneous amplitude and phase respectively. The instantaneous frequency ($\omega(t)$) is obtains from the derivate of the instantaneous phase.

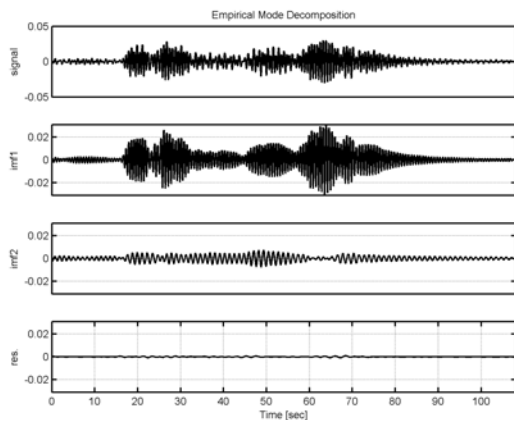


Figure 8: IMF extracted using EMD.

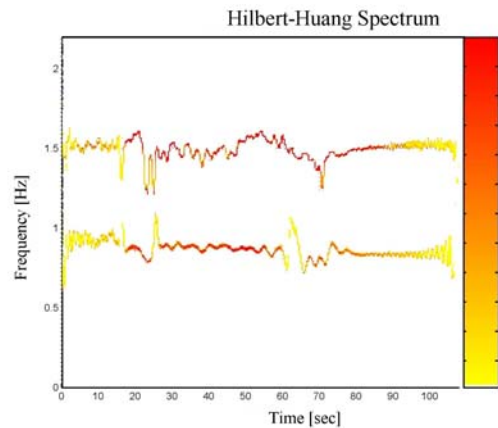


Figure 9: Instantaneous frequency of IMFs.

The EMD process could decomposed a signal $s(t)$, into a finite number of IMFs ($imf_j(t)$, $j=1 \dots n$), and a residue $r(t)$ (Figure 8). Therefore the signal ($s(t)$) could be expressed as a function of amplitude and frequency of the IMFs.

$$s(t) = \sum_{j=1}^n imf_j(t) + r(t) = \sum_{j=1}^n a_j(t) \cdot \cos\left(\int_{-\infty}^t \omega_j(\tau) d\tau\right) + r(t) \quad (4.4)$$

Eq. (4.4) allow us to represent the amplitude and the instantaneous frequency as function of time in a three dimensional plot, in which the amplitude is contoured on the time-frequency plane. This distribution of amplitude is the Hilbert Amplitude Spectrum (HAS), denoted by $H(\omega, t)$ (Figure 9).

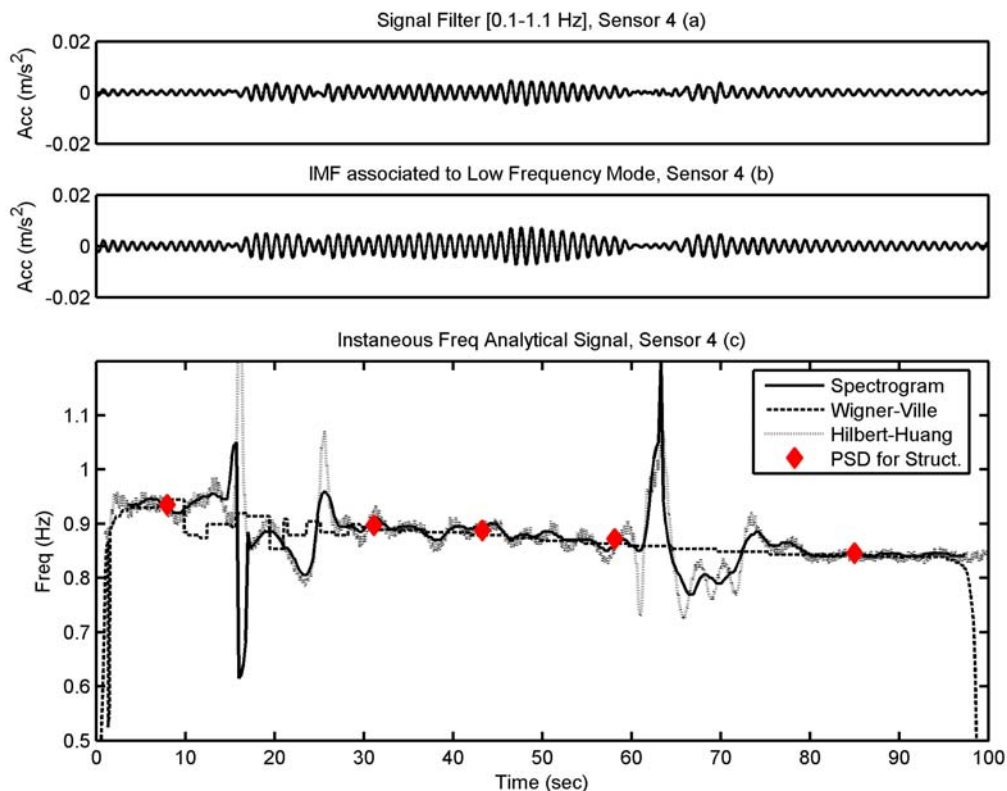


Figure 10: a) Filter Recorded Acceleration. B). IMF associated with low frequency and C) Comparison of Estimates for Predominant Frequency as a Function of Time using Spectrogram, HHT, WVD also shown with red diamonds the values obtained from PSD study with the arm at the different fix extensions.

In Figure 10 all the frequency estimates for the lower predominant frequency are shown. The estimation from the Spectrogram and the Wigner-ville Distribution were obtained by bandpass of the original signal from 0.1 to 1.1 Hz, (Figure 10 (a)). The high frequency variation observed for the Hilbert-Huang transform around second 16 and 70 are due to the low amplitude of the signal. All of the interpretations gave similar results indicating and approximately linear variation of the frequency as a function of arm motion. Analytically it can be shown that the variation is not exactly linear, nevertheless the prediction are consistent.

5. ANALYTICAL REPRESENTATION

An idealized model of the structure formed by two beams was used to additionally validate the results (Figure 11), the mechanical properties of the beams were adjusted, to match the dynamic properties of the actual structure.

The simplified model was excited with a random signal at the base. The non-linear response for the continuously extending the arm was determined by a step by step integration method. Figure 12 and Figure 13 presents the spectrogram and WVD of the signal obtained with the simplified model at the end of telescopic arm. The signal processed by EMD (with intentional interference as discussed in Hernandez (2008) are shown in Figure 14.

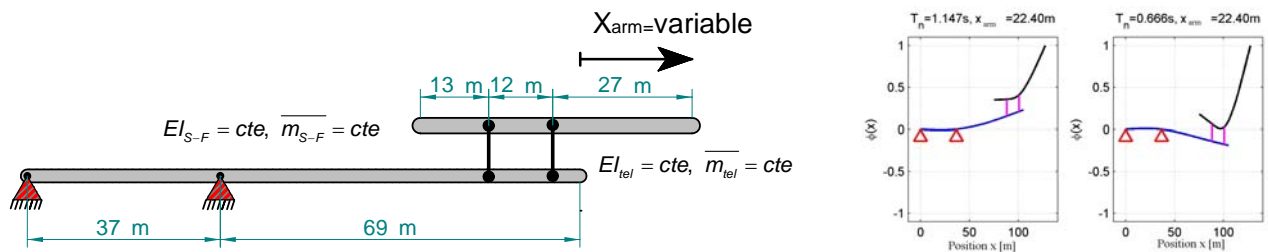


Figure 11: Idealization model and modal shapes.

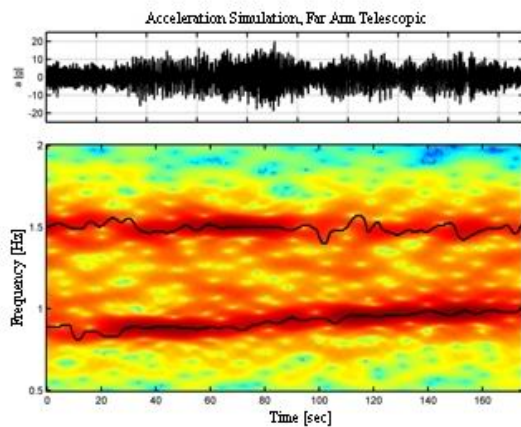


Figure 12: Spectrogram telescopic end arm signal, analytic simplified Model.

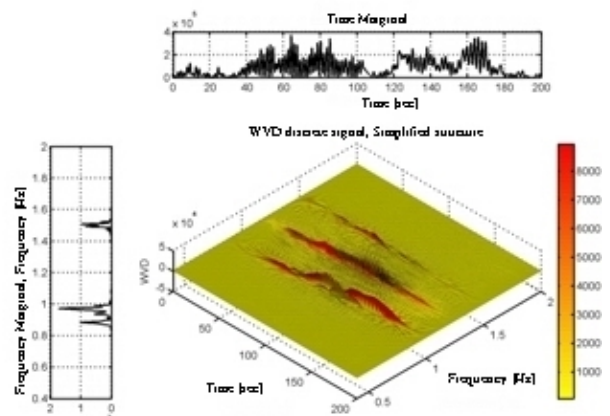


Figure 13: WVD telescopic end arm signal, analytic simplified model.

In Figure 15 the estimate of the prevailing low frequency is presented as identified by the Spectrogram, HHT, WVD and the theoretical model. The match is excellent for all methods.

6. CONCLUSION

1. Despite the rather small frequency variation (11%) in a relative short time (40 seconds) it was possible to detect the change of predominant frequency and to determine with enough accuracy its mean value as a function of time.
2. For this problem the Spectrogram gave a sufficiently reliable description of the frequency change in

- comparison with more mathematically complex and computer demanding procedures.
3. The Wigner-Ville distribution was able to show the predominant frequencies as a function of time but the computational effort was considerable.
 4. The Hilbert-Huang Transform gave comparable good results. It has been shown for this particular case that the modal interference present in the traditional procedure could be reduced under certain restriction by intentional interference procedure.

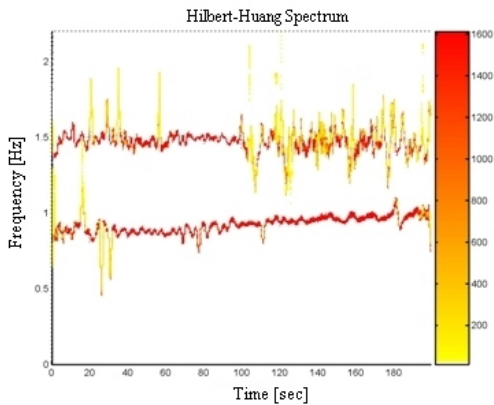


Figure 14: Hilbert Spectrum of heoretical end arm signal response.

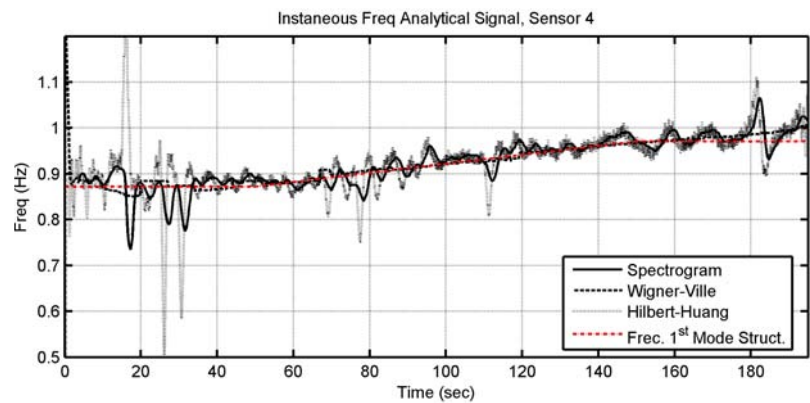


Figure 15: Estimated predominant frequency as a function of time using spectrogram, HHT, WVD for the idialized model.

ACKNOWLEDGEMENTS

The Civil Engineering Department of the University of Chile and the Chilean Council for Research and Technology, CONICYT Fondecyt Project # 1070319 supported this research paper.

REFERENCES

- Boroschek, R. Hernández, F. (2007). Experimental Evaluation of the Modal Parameters Changes of a Telescopic Bulk Dock Structure, Proceeding of the 26ht IMAC.
- Cohen, L. (1995). Time-Frequency Analysis. Prentice Hall.
- Hernandez, F. (2008), Evaluation of Identification Methods for Structures with Changing Dynamic Properties. (Análisis de Métodos de Identificación de Variación de Propiedades Dinámicas de Estructuras). Master Thesis Universidad de Chile. (In Spanish, In Preparation)
- Huang, N., Shen Z., Long S., Wu M, Shih H., Zheng Q., Yen N., Tung C., and Liu H. (1998). The empirical mode decomposition and the Hilbert Spectrum for nonlinear and non-stationary time series analysis. *Proceedings of the Royal Society London; A*, Vol. 454, pp. 903-995.
- Ville J. (1948), Theorie et application de la notion de signal analytique, *Cables et Transmissions*, vol. 2A, pp. 61-74.